Journal of Thermal Analysis and Calorimetry, Vol. 65 (2001) 9–35

THERMODYNAMIC PROPERTIES AND KINETICS OF THE PHYSICAL AGEING OF AMORPHOUS GLUCOSE, FRUCTOSE, AND THEIR MIXTURE

R. Wungtanagorn[1*] *and S. J. Schmidt*[2**]

[1]University of Illinois, Department of Agricultural Engineering, 905 S. Goodwin Ave., Urbana, IL 61801, USA
[2]University of Illinois, Department of Food Science and Human Nutrition, 905 S. Goodwin Ave., Urbana, IL 61801, USA

(Received May 9, 2000)

Abstract

The physical ageing characteristics of glucose, fructose, and their mixtures were studied using standard differential scanning calorimetry (DSC). The inflection, onset, midpoint, half-height, and endpoint glass transition temperature (T_g), fictive temperature (T_f), and relaxation enthalpy (ΔH) were measured as a function of ageing time. The relationship between ΔH and T_f was evaluated. The time dependence of ΔH was fit using the Cowie and Ferguson model. The ageing rate was expressed in terms of the average relaxation time ($<\tau>$) and the entropy production (P). It was found that the fructose component decreased the rate of ageing of the mixtures.

Keywords: Cowie and Ferguson model, DSC, enthalpy relaxation, fructose, glucose, physical ageing

Introduction

Physical ageing is a well known phenomenon in polymer glasses and takes place when a polymer is rapidly cooled from the equilibrium rubber or liquid state into the non-equilibrium glassy state. This non-equilibrium glass will gradually relax towards equilibrium as it is stored below its glass transition temperature [1, 2]. The gradual relaxation of the polymer toward equilibrium is time dependent and manifests itself as changes in thermodynamic properties, such as enthalpy, specific volume, or refractive index, and mechanical properties, such as density [3, 4], brittleness [5, 6], or toughness [5–9], as well as in dielectric properties, such as the dielectric constant and dielectric loss. Changes in these properties over time illustrates the importance of physical ageing in polymers, which for food polymers relates to the shelf life and stability of food products during storage, use, and consumption.

---

[*] Phone: (217) 333-3196, E-mail: wungtana@uiuc.edu
[**] Phone: (217) 333-1324 or (217) 333-1326, E-mail: sjs@uiuc.edu

1418–2874/2001/ $ 5.00

Akadémiai Kiadó, Budapest
Kluwer Academic Publishers, Dordrecht

Because of the practical difficulties of measuring volume relaxation in polymer glasses, enthalpy relaxation measurement is another practical choice which is conveniently carried out using a standard differential scanning calorimeter (DSC) [10]. A decrease in enthalpy as a result of the relaxation process can be analyzed as an enthalpy recovery peak (also referred to as T_g overshoot) during a heating DSC scan. The intensity and the position of the enthalpy recovery peak depends on both the nature of the sample and how the sample was prepared, i.e., its thermal history.

Many processes used in the preparation of food products such as dehydration, concentration, extrusion, or melting transform the sugar components into amorphous non-equilibrium glasses. Food processes involving a quench from a high (or melt) temperature above the glass transition to a temperature below the glass transition create the suitable thermal history for initiation of physical ageing. Like typical amorphous polymers, amorphous sugars or sugar containing products, such as hard candy and low moisture foods, can undergo physical ageing during storage below their glass transition temperatures. Therefore, physical ageing may cause the unfavorable alteration of structure, texture, sensory and eventually quality, stability and shelf life of those products.

Although physical ageing has been studied extensively in polymers, only a few studies involving simple sugars have been reported: maltose [11, 12], and sucrose [13–16]. Besides sugars, physical ageing has also been studied in glassy flour containing foods, such as low moisture white bread and extruded bread [17]. However, most sugar containing products are composed of a mixture of sugars. This study is focused on the physical ageing of two common simple sugars: fructose and glucose.

The objectives of this research were: 1. to monitor changes, as a function of ageing time, of the heat capacity, glass transition temperature (T_g), fictive temperature (T_f), and relaxation enthalpy (ΔH) as a consequence of physical ageing in individual sugars and sugar mixtures. The systems studied were glucose, fructose, and three binary mixtures (75/25, 50/50, and 25/75 mass ratios of glucose to fructose). The ageing temperatures (T_a) were 10°C below the glass transition temperatures (T_g midpoints) and an additional T_a of 20°C below the T_g midpoint for the 50/50 ratio, and 2. to evaluate the kinetics of physical ageing in glucose, fructose, and their mixtures using the Cowie and Ferguson (CF) model. The ageing rates (also referred to as relaxation rates) of the sugars were expressed in terms of the average relaxation times ($<\tau>$) and entropy production (P). These parameters were calculated using the CF model parameters.

Materials and methods

Materials, sample preparation, and instrumentation

D(–)Fructose (*D*-Levulose) (Product No. G-2543, SigmaUltra grade) and Anhydrous *D*-(+)-Glucose (Product No. G-7528, SigmaUltra grade) were obtained from Sigma Chemical Company (St. Louis, MO), and were used without further purification.

In order to obtain uniform mixing for the glucose-fructose mixtures, similar particle sizes for both sugars were preferred. This was done by screening each sugar through various sieves (3′′ stainless frame with stainless cloth, W. S. Tyler, Mentor, Ohio) from No. 60 (opening of 0.250 μm) to No. 100 (opening of 0.150 μm). The size of the sugar particles collected were between 0.180 (No. 80) and 0.212 (No. 70) micrometers. After the screening process, the glucose and fructose samples were dried individually in a vacuum oven at 60°C and 14.7 psi for 12 h. The dried glucose and fructose were then weighted at three mass ratios of glucose to fructose, 75/25, 50/50, and 25/75 (denoted as 75/25 GF, 50/50 GF, and 25/75 GF, respectively) and mixed by shaking in a glass bottle for approximately 30 min. The mixing was performed with a total mass of about 40 g.

The sugar mixtures were analyzed for moisture content (duplicate determination) by Karl–Fischer titration [18] and for the glucose-fructose mass ratio (triplicate determination) by HPLC. The results are shown in Table 1.

Table 1 The moisture content and glucose–fructose mass ratio analysis of glucose, fructose, and their mixtures

Glucose–fructose mass ratio prepared by weighing	Moisture content by Karl–Fischer titration/ mg water g^{-1} total	Glucose–fructose mass ratio analyzed by HPLC
100/0	0.346±0.035	–
75/25	0.318±0.011	74.18/25.82±0.006
50/50	0.263±0.012	47.99/52.01±0.018
25/75	0.232±0.013	24.61/75.39±0.016
0/100	0.246±0.017	–

Residual machine oil remaining from the manufacturing of the DSC pans (pan part number 900793.901, and lid part number 900794.901, TA Instruments, Inc., New Castle, DE) was removed by sonicating the pans in acetone for 30 min, wrapping with paper towels, and drying at ambient temperature overnight. The sugar crystals and sugar crystal mixtures (10±0.1 mg) were weighed into acetone washed aluminum DSC pans, and hermetically sealed. In order to obtain the maximum temperature control, all samples experienced the entire thermal history in the DSC throughout each experiment. All pans were re-weighed after each DSC experiment to ensure that there was no mass loss due to pan leakage problems.

A TA Instrument 2920 MDSC (TA Instruments, Inc., New Castle, DE), equipped with a refrigerated cooling accessory, Universal Analysis software and Thermal Analysis-Heat Capacity software, was used. Dry helium was used as the purged gas through the sample cell at a rate of 25 $cm^3 min^{-1}$. Dry nitrogen gas was used to purge the refrigerated cooling accessory during heating and dry helium gas was used during cooling in order to achieve the highest efficiency of cooling. The flow rate of both gases was 150 $cm^3 min^{-1}$.

Indium (900902.901, TA Instruments, Inc., New Castle, DE) was used for cell constant and temperature calibrations, and sapphire (part number 915079.902, TA Instruments, Inc., New Castle, DE) was used for heat capacity calibration. An empty, sealed uncoated aluminum DSC pan was used as the reference pan and both the reference and sample pans were matched in mass to within 0.05 mg.

The melting points of glucose and fructose measured by the DSC (at a heating of 10°C min^{-1}) were 158.24±0.106°C (onset), 163.92±0.262°C (peak); and 113.58±0.318°C (onset), 132.03±1.018°C (peak), respectively. The melting point of glucose was reported at 143°C (onset) and 158°C (peak) [19], 135°C (onset) and 150°C (peak) [20], 158°C [21], and 150°C [22]. Also, the melting point of fructose was reported at 108°C (onset) and 127°C (peak) [19], 80°C (onset) and 115°C (peak) [20], 124°C [21], 104.6°C [23], and 103°C [22]. The values obtained in this present study were higher than the literature values.

Thermal history

Figure 1 shows the schematic diagram of enthalpy and heat capacity changes of a sample subjected to the following thermal cycles. The sugar crystals were initially melted in the DSC pan by heating from ambient temperature to 168°C at a heating

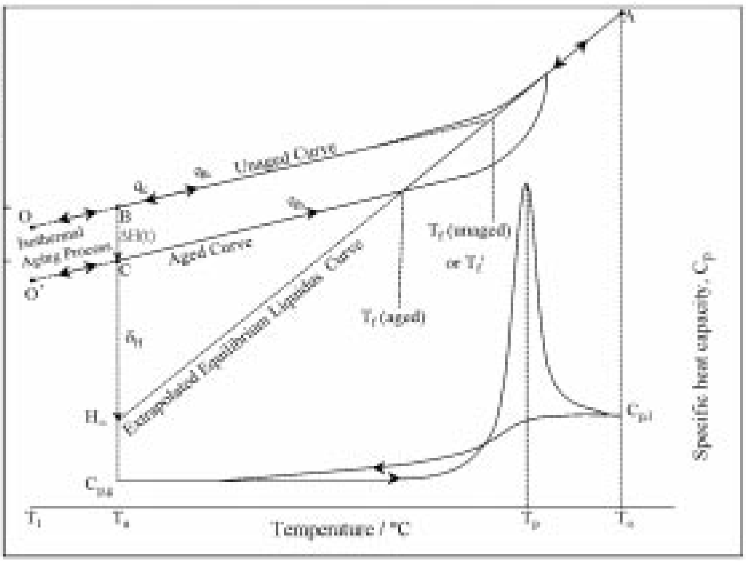

Fig. 1 Schematic diagram of the change in enthalpy and specific heat capacity of glucose, fructose, and their mixtures with isothermal ageing at T_a (path ABCO′CA) and without ageing (path ABOBA). The samples were cooled at a cooling rate q_c and heated at a heating rate q_h. H_i and $H(t)$ are the enthalpies at the beginning of ageing and at ageing for time t, respectively. The equilibrium enthalpy at ageing temperature T_a is H_∞. $C_{p,l}$ is the specific heat capacity of the equilibrium liquid and $C_{p,g}$ is that of the glass. T_f(unaged) and T_f(aged) are the fictive temperatures of unaged and aged samples, respectively. $\Delta H(t)=H_i-H(t)$ and $\delta H=H(t)-H_\infty$, respectively. T_p denotes the maximum peak of the heat capacity curve during reheating scan through the glass transition region

rate (q_h) of 10°C min^{-1} and held for 0.3 min. The combination of the temperature and the holding time was optimized to ensure complete melting of the sugar crystals and, at the same time, to minimize sugar decomposition. However, slight browning of the fructose only samples was observed. The molten sugar was then cooled at a cooling rate (q_c) of 10°C min^{-1} to an ageing temperature T_a (path AB) in order to form an amorphous glass and was held for various ageing times [t_a; 5 to 10 080 min (7 days)]. As a result of ageing, the enthalpy of the sample decreases from H_i to $H(t)$ (path BC; $\Delta H(t)$). An ageing temperature was chosen at temperatures about 10°C below the T_g midpoint. An additional T_a at a temperature 20°C below the T_g midpoint was also used for the 50/50 ratio. After ageing, the sample was again cooled to a temperature of about 55°C below its T_g midpoint and was equilibrated for 3 min (path CO′). During this step, it was assumed that no appreciable relaxation occurred during cooling of the aged sample to T_1 [24] and that the specific heat capacity of the material was independent of ageing time, i.e., the line CO′ is parallel to the line BO [25]. The sample was then immediately scanned to 120°C at a q_h of 10°C min^{-1} (path O′CA). In order to erase the effect of the previous thermal history, the sample was kept at 120°C, instead of 168°C to prevent any additional decomposition, for 10 min. A second scan was done on the same sample by cooling at a q_c of 10°C min^{-1} to the starting temperature (55°C below its T_g midpoint) (path ABO), then the sample was immediately reheated at a q_h of 10°C min^{-1} (path OBA) to obtain an unaged (reference) rescan curve.

Samples with ageing times from 5 to 360 min were done in duplicate; whereas samples with longer ageing times (480 to 10 080 min) were only done once.

Heat capacity values were measured using the Thermal Solution-Heat Capacity Analysis software [26] for aged, and unaged sugar glasses between 55°C below the T_g midpoint and 120°C at temperature intervals of 0.1°C.

Determination of T_g values

The glass transition temperatures were determined using the Universal Analysis software [27]. The program fits three tangent lines to the DSC curve within a specified temperature limit, then determines the glass transitions as: T_g onset – the temperature at the intersection of the regression line from the starting point of the specified limit (the first tangent) and the inflection tangent of the step change (second tangent); T_g inflection – the temperature at the steepest slope on the DSC curve between the first tangent and the regression line after the transition (the third tangent); T_g half-height – the temperature at the total heat flow value halfway between the value at onset and the value at end point of the transition region; T_g midpoint – the mid-temperature between T_g onset and T_g endpoint; and T_g endpoint – the temperature at the intersection of the inflection tangent and the third tangent.

Enthalpy measurement

The relaxation enthalpy or enthalpy loss, ΔH (J g^{-1}), between an aged and an unaged rescan sample can be calculated using Eq. (1) [28]:

$$\Delta H = \int_{T_0}^{T_1} (C_{\mathrm{p,aged}} - C_{\mathrm{p,unaged}})\,\mathrm{d}T \qquad (1)$$

where $C_{\mathrm{p,aged}}$ and $C_{\mathrm{p,unaged}}$ are the specific heat capacities of the aged and unaged samples, respectively, and T_0 is a temperature well above T_g and T_1 is a temperature well below T_g. ΔH can also be obtained by using the relationship between C_p and the power output, P [25]. The output power is directly proportional to the C_p of the sample by $C_p=P/(qm)$, where m is the dry mass of the sample and q is the heating rate. By assuming the sample is heated at the same rate as the furnace, the relaxation can be obtained by subtracting the unaged heat flow curve, P_{unaged}, from the aged heat flow curve, P_{aged}, and integrating the difference in area between the two curves using Eq. (2):

$$\Delta H = \frac{1}{m}\int_{t_1}^{t_0} (P_{\mathrm{aged}} - P_{\mathrm{unaged}})\,\mathrm{d}t \qquad (2)$$

where t_1 and t_0 are the times corresponding to temperatures T_1 and T_0, respectively.

Determination of fictive temperature (T_f)

Fictive temperature (T_f) is defined as the temperature at which the enthalpy of a material will be equal to the equilibrium enthalpy if it was instantaneously moved to that temperature at a constant pressure [29–31]. T_f was calculated as the intersection of the enthalpy-temperature curves for the glass and liquid states, using the method of Richardson and Savill [32]. The enthalpy ($H_{\mathrm{glass}}(T)$ and $H_{\mathrm{liquid}}(T)$) at each temperature was obtained by integrating the heat capacity curves in the glass ($C_{\mathrm{p,g}}$) and liquid ($C_{\mathrm{p,l}}$) regions. $C_{\mathrm{p,g}}$ and $C_{\mathrm{p,l}}$ are defined as linear functions of temperature, i.e., $C_{\mathrm{p,g}}(T)=a+bT$ and $C_{\mathrm{p,l}}=A+BT$ where a, b, A, and B are constants obtained from linear least square fitting to the linear regions of the glass and liquid heat capacities. T_f for aged and unaged samples is defined as the temperature at which the equations for $H_{\mathrm{glass}}(T)$ and $H_{\mathrm{liquid}}(T)$ intersect, i.e., $H_{\mathrm{glass}}(T)$ and $H_{\mathrm{liquid}}(T)$ were set to be equal and T_f is the solution of the quadratic equation.

Results and discussion

Evaluation of ΔC_p

ΔC_p is the difference between the linear extrapolated glass ($C_{\mathrm{p,g}}$) and the liquid ($C_{\mathrm{p,l}}$) heat capacity curves of the sample at T_g midpoint. The approximate temperature ranges used for the linear glass and liquid regions are reported in Table 2, as well as, the average unaged ΔC_p and the average aged ΔC_p values. The average unaged ΔC_p values were obtained by analyzing all of the unaged (reference) DSC curves. All the aged ΔC_p values within each sugar were very similar and showed no trend over time.

Thus, an average aged ΔC_p value for each sugar was obtained by analyzing its aged DSC curves over all ageing times.

Table 2 The average ΔC_p values of glucose, 75/25, 50/50, 25/75 mass ratios of glucose to fructose, and fructose. The values of the unaged average ΔC_p were analyzed using all of the unaged (reference) DSC curves, whereas, the valves of the average aged ΔC_p were analyzed using all of the aged DSC curves of the aged samples over all ageing times. C_p glass ranges and C_p liquid ranges were the approximate temperature ranges used for linear least square fitting in the glass and liquid regions using the method of Richardson and Savill [32]

Sugars	C_p glass temperature range/°C	C_p liquid temperature range/°C	Average unaged ΔC_p/ J g^{-1} °C^{-1}	Average aged ΔC_p/ J g^{-1} °C^{-1}
Glucose (T_a 28.0°C)	–6 to 20	55 to 80	0.77±0.022	0.77±0.027
75/25 GF (T_a 16.5°C)	–18 to 10	45 to 70	0.75±0.020	0.77±0.023
50/50 GF (T_a 9.5°C)	–23 to 5	42 to 60	0.78±0.018	0.80±0.012
50/50 GF (T_a –0.5°C)	–23 to 5	42 to 60	0.79±0.010	0.81±0.014
25/75 GF (T_a 4.5°C)	–32 to –5	35 to 55	0.77±0.015	0.81±0.019
Fructose (T_a –2.0°C)	–38 to –15	30 to 45	0.77±0.014	0.81±0.021

The results showed that the average unaged ΔC_p values of glucose, fructose and the three mass ratios of glucose to fructose were very similar. Literature ΔC_p values of glucose and fructose are given in Table 3. Orford *et al.* [33] reported that the ΔC_p values for glucose and fructose were very close at 0.84 and 0.88 J g^{-1} °C^{-1}, respectively, which is the same trend observed in this research (Table 2). The ΔC_p value obtained for glucose is lower than the value reported by Orford *et al.* [33], but higher than the value of 0.63 J g^{-1} °C^{-1} reported by Roos [19]. The value of ΔC_p for fructose; however, was similar to that reported by Roos [19] at 0.75 J g^{-1} °C^{-1} and Fan and Angell [23] at 0.74 J g^{-1} °C^{-1}, but lower than the value reported by Orford *et al.* [33] of 0.88 J g^{-1} °C^{-1}.

The results also showed that the average aged ΔC_p values of glucose, fructose and the three mass ratios of glucose to fructose were very similar. However, the values of ΔC_p aged were slightly higher than the unaged values but had similar standard deviations (±0.01 to ±0.03). The average aged ΔC_p values for all the sugars were in the range of 0.77 to 0.81 J g^{-1} °C^{-1}, which is in the range of the literature values for the pure components (0.63 to 0.88 J g^{-1} °C^{-1}).

Glass transition temperature (T_g)

Unaged sugars

The values of T_g onset, T_g half-height, T_g midpoint, T_g inflection, and T_g endpoint for unaged samples are reported in Table 4. A single value T_g for each sugar mixture was found, indicating good miscibility between the two molten sugars. In agreement with Finegold *et al.* [34], fructose shows the role of a diluent or plasticizer in the mixtures, because it depresses the T_g of glucose, i.e., T_g values of the mixtures decreased as the

Table 3 Glass transition temperatures, T_g, and the change in heat capacity occurring over the glass transition, ΔC_p, of glucose and fructose and 1:1 mass/mass of glucose to fructose

T_g/°C			C_p/J g^{-1} °C^{-1}			Thermal history
Glucose	1:1 mass/mass G:F	Fructose	Glucose	1:1 mass/mass G:F	Fructose	
31^a, 36^b, 41^c	13.0^b	5^a, 10^b, 16^c	0.63		0.75	no indicated cooling rate, heated at 5°C min^{-1} [19]
38^d (31^d)		7^d	0.88		0.84	cooled at 50°C min^{-1} after melt, and reheated at 10 (and 1.25) °C min^{-1} [33, 65]
39^b	21^b	13^b	0.57	0.58	0.46	melted and quenched in an aluminum foil under nitrogen shroud and heated in DSC at 10°C min^{-1} [34]
31^d		11^d & 100^d				no indicated cooling rate, heated at 10°C min^{-1} [21]
31^e, 34^e, 30^e		16^e, 10^e, 30^e				estimated T_g at 10^{12} Pa from parameters obtained from the VTF, power law and WLF equations, respectively. The parameters of the equations obtained from fitting the viscosity data [66]

[a] T_g onset, [b] T_g midpoint, [c] T_g endpoint, [d] unidentified T_g but probably is T_g midpoint, [e] calculated T_g from viscosity data.

content of fructose increased. The glass transition range (T_g endpoint minus T_g onset) was smallest for pure glucose (4.28°C) and increased with increasing fructose content, with the largest glass transition range value being that for pure fructose (9.08°C).

Table 4 The glass transition of unaged glucose, 75/25 GF, 50/50 GF at two ageing temperatures (T_a) of 9.5°C and –0.5°C, 25/75 GF, and fructose. The T_g onset, half-height, midpoint, inflection, and endpoint were analyzed from the total heat flow by using the Universal Analysis software [27]. T_g range is the difference between T_g endpoint and T_g onset. The limiting fictive temperature T_f' (i.e., T_f of unaged sample) was obtained using the method of Richardson and Savill [32]. Calculated T_g midpoint was obtained using Eq. (3)

Temperature/°C	Glucose	75/25 GF	50/50 GF	50/50 GF	25/75 GF	Fructose
T_g onset	35.80 ±0.778	23.65 ±0.919	16.62 ±1.387	15.30 ±0.647	9.30 ±1.314	2.25 ±0.996
T_g half-height	37.73 ±0.718	26.58 ±0.816	20.17 ±1.457	18.94 ±0.575	13.29 ±1.198	6.82 ±1.275
T_g midpoint	37.94 ±0.728	26.70 ±0.829	20.25 ±1.418	18.97 ±0.590	13.11 ±1.444	6.79 ±1.066
T_g inflection	39.66 ±0.749	28.53 ±0.894	21.77 ±1.371	20.54 ±0.637	14.79 ±1.242	8.29 ±0.913
T_g endpoint	40.08 ±0.715	29.76 ±0.761	23.88 ±1.476	22.63 ±0.565	17.39 ±1.178	11.33 ±1.184
T_g range	4.28	6.11	7.26	7.33	8.09	9.08
$T_{f,unaged}$ (T_f')	35.08 ±0.756	24.44 ±0.668	18.26 ±1.470	17.02 ±0.606	11.44 ±1.351	4.62 ±1.287
T_a	28.0	16.5	9.5	–0.5	4.5	–2.0
T_g midpoint–T_a	9.89	10.14	10.75	19.47	8.61	8.79
T_f'–T_a	7.08	7.94	8.76	17.52	6.94	6.62
Calculated T_g midpoint	–	30.15	22.37	22.37	14.58	–

The calculated T_g midpoint values for the sugar mixtures were calculated using the Couchman–Karasz equation (Eq. (3)) and are given in Table 4 [35]:

$$T_g = \frac{\Delta C_{p_1} W_1 T_{g_1} + \Delta C_{p_2} W_2 T_{g_2}}{\Delta C_{p_1} W_1 + \Delta C_{p_2} W_2} \tag{3}$$

where subscripts 1 and 2 refer to the glucose and fructose components, respectively. W is the mass fraction of each component. The values used for ΔC_{p_1} and ΔC_{p_2} were the average unaged values for pure glucose and pure fructose from Table 2 (0.77 J g^{-1} °C^{-1}). The values used for T_{g_1} and T_{g_2} were the T_g midpoint of pure glucose (37.94°C) and pure fructose (6.79°C), which are reported in Table 4. As shown in Table 4, the calculated T_g values were larger than the T_g midpoint values obtained from the DSC curves, and in the 75/25 GF case, larger than the T_g endpoint value.

T_g values reported by others are shown in Table 3. The T_g onset to endpoint values ranged from 30 to 41°C for glucose and from 5 to 30°C for fructose. The variation among the reported T_g values is greater for fructose than for glucose. The T_g values of glucose from this study are in the range reported in the literatures, however those of fructose are slightly lower than the values reported by others. The difference in T_g values between the reports is probably due to several factors, such as the initial moisture content of the samples before melting, the moisture content of the glassy sugars after melting and cooling, the method used to form the sugar glasses (i.e., rate of cooling, water loss, etc.), and the method used to determine and report the T_g values [12].

It should be noted that the previous thermal history and the decomposition of the molten fructose may also be responsible for the differences in T_g values. Fan and Angell [23] carried out an experiment on fructose exposing it to three different thermal histories. A 'partial melt' was prepared by heating crystalline fructose to its melting point at 104.6°C for less than the time needed for complete melting. A 'fresh melt' was prepared by melting the crystalline fructose to its melting point and allowing the crystals to melt completely. However, in order to prevent decomposition after melting was completed, the sample was cooled immediately to below 87°C. A 'relaxed melt' was prepared in the same way as the fresh melt, but after melting tautomer equilibration was allowed to occur at a temperature (98.9°C for 2.5 h) low enough that negligible chemical decomposition was permitted. The T_g value of the partial melt (T_g onset≈16°C) was higher than the value of the fresh melt (T_g onset ≈13°C) and was much higher than the relaxed melt (T_g onset≈7.2°C). T_g decreased as the extent of decomposition of the molten fructose increased. The T_g onset of fructose in this paper was 2.25°C which is also lower than T_g onset of the fresh melt found by Fan and Angell [23]. Therefore, the lower values of T_g for fructose in this research compared to those in the literature may be due to the thermal history used for melting the sugars and the degree of decomposition of fructose.

In order to show that decomposition affects the T_g values, the amorphous fructose sample in this research was also prepared by melting the fructose crystals at 150°C, then cooling to –25°C. The unaged DSC curve was obtained by immediately reheating the sample. All heating and cooling rates were at 10°C min^{-1}. Browning of the fructose only sample was not observed for this thermal history. The T_g onset, half-height, midpoint, inflection, and endpoint were 7.57±0.343, 10.28±0.381, 10.40±0.373, 12.13±0.367, 13.22±0.437°C, respectively. These fructose only T_g values are higher than those reported in Table 4 and are closer to those reported in the literature (Table 3).

Moreover, the situation is more complex in the case of pure fructose or fructose mixtures than in the case of pure glucose. Amorphous fructose not only shows a major transition (i.e., the glass transition) but also multiple transitions in the liquid state above the glass transition [23]. The multiple transitions are slow relaxation processes in the liquid state. A transition above T_g was reported earlier by Slade and Levine [21], at about 100°C which was considered as a glass transition temperature. Finegold *et al.* [34] also reported that there was a high-temperature relaxation process, which was also observed for galactose, but not for glucose, xylose or mannose. The amplitude of the step change in heat capacity at 100°C was only one-fourth of that at 13°C (the actual T_g midpoint) and decreased with repeating thermal cyclings. Moreover, the high-temperature relaxation process could be removed by adding glucose, but not sucrose, to fructose [34]. Interestingly, Fan and Angell [23] reported that a small high-temperature transition also occurred in glucose at around 87°C. This small high-temperature transition in glucose was not observed in this research.

Fan and Angell [23] studied fructose further and found that, beside the major glass transition, three other transitions above T_g were also present, a smaller transition (denoted as T_1) at 51°C (onset), a larger transition (denoted as T_2) at 94°C (onset), and a third transition (denoted as T_3) at 122°C (onset), with ΔC_p values of 0.43, 0.093, and 0.055 J g^{-1} °C^{-1}, respectively. The values of ΔC_p at T_1, T_2 and T_3 are about 60, 13 and 7.5% of the ΔC_p at T_g (0.75 J g^{-1} °C^{-1}), respectively. The T_3 transition was observed when a melt experienced five heating (above 137°C)-cooling cycles. In addition, if the melt was annealed at a temperature between T_g and T_2 for a period of time, a T_2 overshoot similar to the T_g overshoot, was also observed. According to Fan and Angell [23], the complexity of the molten state of fructose is due to: 1) the initial non-equilibrium state obtained on melting, i.e., at least six distinct species coexist: the two anomeric forms (α and β) of each of the $^1C_4$ and $^4C_1$ fructopyranose and of the fructofuranose, 2) the consequence of the decomposition processes around the melting point, and 3) the temperature dependence of the equilibrium state of the liquid, i.e., the composition of the tautomers and the conversion kinetics among the tautomers depend on temperature.

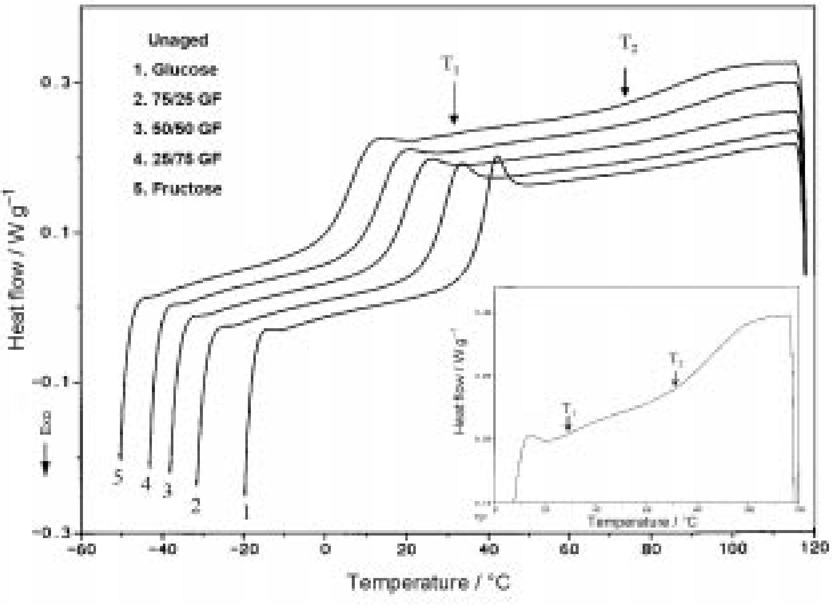

Fig. 2 DSC heating scan of the unaged samples for glucose, fructose and their mixtures at a heating rate of 10°C min^{-1}. T_1 and T_2 on the unaged fructose DSC curve are the high-temperature transitions (details in text). The insert highlights the T_1 and T_2 transitions for pure unaged fructose

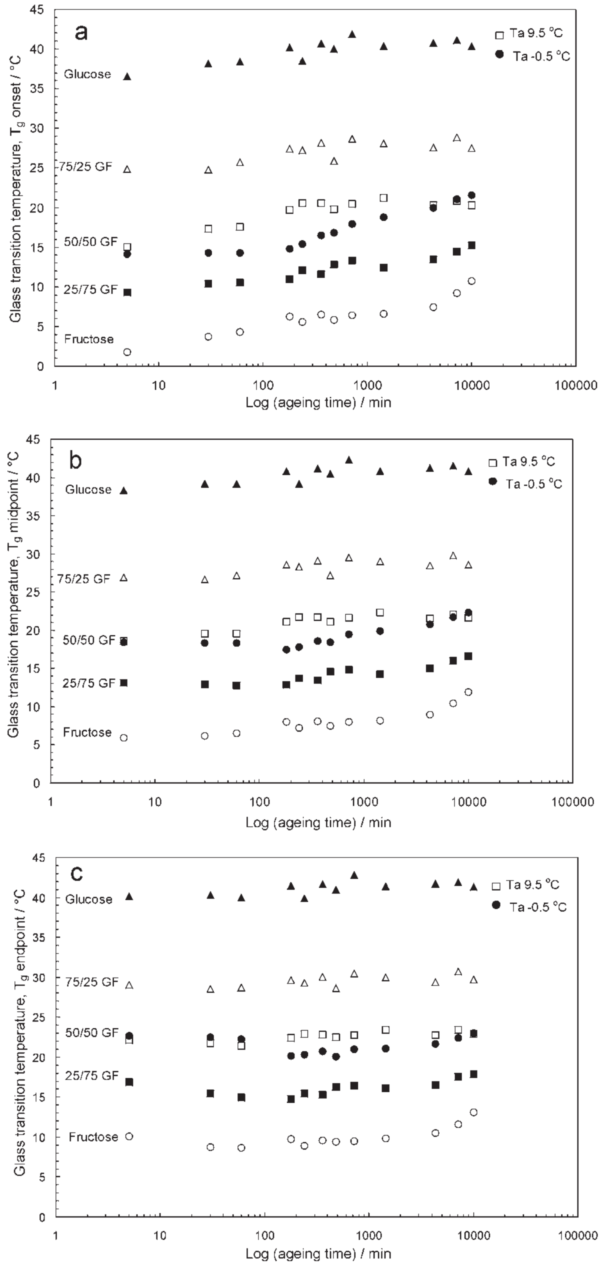

Fig. 3 The glass transition temperatures analyzed from total heat flow for glucose, fructose, and three mass ratios of glucose to fructose; 75/25, 50/50 at two ageing temperatures (9.5 and –0.5°C), and 25/75 as a function of ageing time a – T_g onset, b – T_g midpoint, and c – T_g endpoint

Our research confirmed the existence of both high-temperature transitions T_1 (T_1 onset 31.82±2.699°C, T_1 midpoint 34.176±1.320°C) and T_2 (T_2 onset 71.57±1.430°C, T_2 midpoint 85.19±0.772°C), in the case of fructose (Fig. 2, molten at 168°C). However, the T_1 transition was not very noticeable and was difficult to observe in the sugar-mixture DSC curves. The values of T_1 and T_2 are lower than those reported by Fan and Angell [23]. The lower T_1 and T_2 values reported in this research may be due to the decomposition of fructose and the difficulty in determining T_1 and T_2 due to the small transition steps. By melting the fructose crystals from room temperature to 150°C (10°C min^{-1}) in order to prevent decomposition of fructose, then cooling to –25°C (10°C min^{-1}), T_1 and T_2 were found at 46.73±1.985 (onset), 48.88±3.598 (midpoint), and 90.74±1.718 (onset), 101.11±1.287 (midpoint) °C, respectively. Both T_1 and T_2 obtained from melting at 150°C were higher than those obtained from melting at 168°C and were closer to those reported by Fan and Angell [23].

In addition, it was observed that the T_2 transition step, which was not observed in glucose, was reduced with increasing glucose content (Fig. 2). It was not clear whether the decrease in magnitude of the T_2 transition is due to the decrease in fructose content, or to the decrease in magnitude of T_2 is because glucose is involved in the T_2 relaxation process of fructose. Finegold *et al.* [34] also reported a decrease in magnitude of T_2 in fructose with increasing glucose content.

The high-temperature transitions in fructose and glucose-fructose mixture samples interfered with the determination of the linear region above T_g. This may have caused the slightly higher ΔC_p of the aged compared to the unaged samples (Table 2).

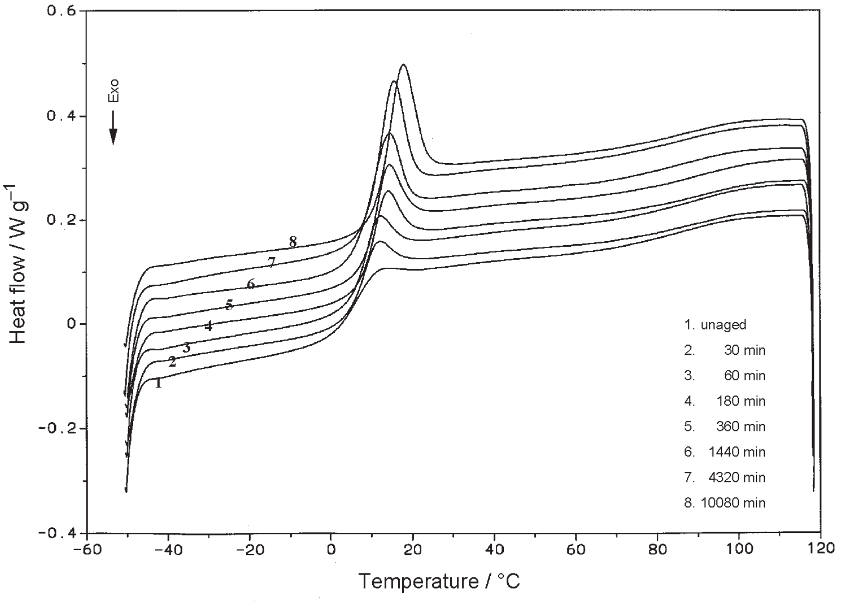

Fig. 4 DSC curves of an unaged and aged fructose glasses at various ageing times, fructose aged at –2°C

Aged sugars

The T_g values were also determined for aged samples. The onset, midpoint and endpoint T_g values were plotted as a function of $\log_{10}$ of the ageing time and are shown in Figs 3a to 3c. The T_g half-height and inflection plots are given in Wungtanagorn [36]. An example standard DSC heating curves for fructose is shown in Fig. 4. All sugars exhibited similar heating curves (other curves are given in Wungtanagorn [36]), except for the presence of high-temperature relaxations above the glass transition temperature for fructose and fructose mixtures. The magnitude of these high-temperature relaxations decreased as the glucose content increases, which was discussed previously. As fructose was aged at –2.0°C for 5 min to 7 days, the magnitude of the T_g overshoot at the major transition (i.e., at T_g of 6.79°C for unaged fructose) increased, while the high-temperature T_2 transition was still observed and the magnitude of the T_2 transition appeared to be unchanged as the T_g overshoot increased (Fig. 4). ageing below the glass transition temperature, therefore, may not affect the T_2 transition, which is in agreement with Fan and Angell [23]. However, Fan and Angel [23] reported further that annealing fructose relaxed melts at 23°C (between T_g and T_2) would increase the T_g as much as ~6°C and decrease T_2 as much as ~15°C.

As observed in Figs 3a to 3c, the measured T_g values were affected by ageing. The overall T_g onset, inflection, midpoint, and endpoint of each sample increased slightly as a function of ageing time. However, theoretically the value of T_g is ex-

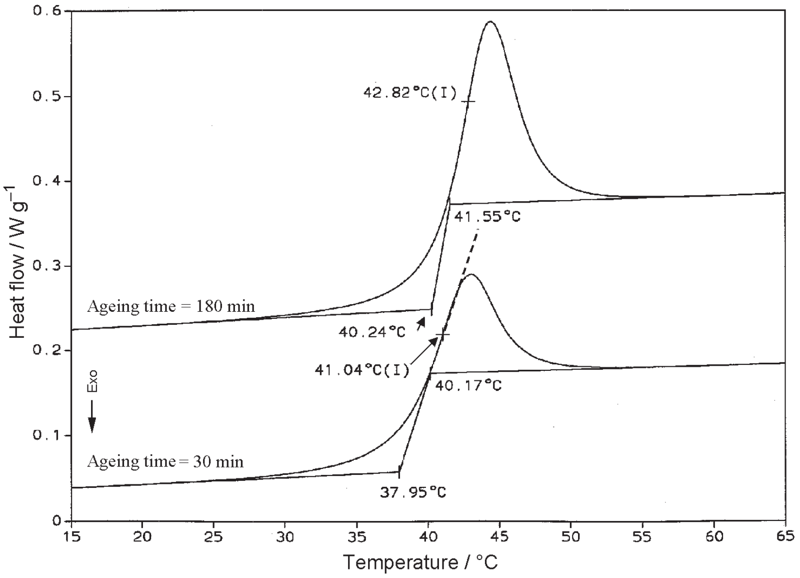

Fig. 5 Glucose DSC curves aged at 28°C for 30 and 180 min. The dashed line in the 30 min aged curve was extended from the inflection tangent line (second tangent) so that the difference in the slopes of both inflection tangent lines (30 min *vs.* 180 min sample) can be compared

pected to decrease as ageing time increases (T_g decreases as ΔH increases, Fig. 1). This increase in the software-measured T_g with ageing time is the result of two factors. First, the T_g overshoot peak becomes higher and steeper with ageing time due to the increase in enthalpy relaxation. Secondly, the peak of the T_g overshoot is shifted along the x axis as ageing time increases. These two factors account for the increase in T_g with ageing time due to the way that T_g values are determined using the Universal Analysis Software. All T_g values obtained using the Universal Analysis software are determined from the intersections of the first, second, and third tangents as described in the methods section. The change in the second tangent controls the T_g values obtained. If the second tangent is steeper, the intersection of the first and the second tangents will shift to a higher temperature and therefore the T_g onset values for the longer ageing times are larger than for the shorter ageing times (Fig. 5). However, the intersection of the third tangent and the second tangent, which determines the T_g endpoint, shifts to a lower temperature as the peak becomes steeper. In this case, the T_g endpoint values for the long ageing times are still slightly higher than that for the shorter ageing times because the endotherm is not only higher and steeper but also shifts to a higher temperature as the ageing time increases. Therefore, the T_g values obtained using the software increased as ageing time increased. However, a decrease in T_g is obtained (corresponding to theory) if we consider the calculated T_g instead of the software-measured T_g. The calculated T_g is determined from the intersection of the extrapolated glassy and liquid enthalpy curves (where T_g calculated is now referred to as T_f). T_f is discussed in detail below.

In addition, all T_g values decreased with increasing fructose content. For 50/50 GF glasses, the values of T_g onset, midpoint, and endpoint of the samples aged at an ageing temperature of 9.5°C were higher than those aged at an ageing temperature of –0.5°C. A narrowing of the glass transition range (T_g endpoint (data in Fig. 3c) minus T_g onset (data in Fig. 3a)) for all mixtures as ageing time increased was observed. The glass transition range decreased from 3.56 (glucose), 4.16 (75/25 GF), 7.11 (aged 9.5°C, 50/50 GF), 8.56 (aged –0.5°C, 50/50 GF), 7.55 (25/75 GF), 8.24 (fructose)°C for the 5 min-aged samples to 0.956, 2.18, 2.62, 1.37, 2.71, 2.36°C for the 7 day-aged samples, respectively. The slight overall increase in T_g as a function of time and the narrowing of the glass transition region were also observed in maltose glasses [11].

Fictive temperature (T_f)

Unaged sugars

The method of Richardson and Savill [32] was employed to determine the fictive temperature, T_f. Theoretically, in the liquid state at equilibrium, T_f is equal to T, and T_f=T_g onset when the material transitions to the glassy state. Once the material is aged, the T_f of the aged sample is lower than the T_g onset of the unaged sample and T_f of an aged material at equilibrium is equal to T_a. The T_f of the unaged sample is, therefore, the upper limit of the T_f for the aged sample in the glassy state. The T_f of an unaged sample is denoted as the limiting fictive temperature, T_f'. The T_f' obtained for all unaged DSC curves for each sample are given in Table 4. The values of T_g onset obtained from the Universal Analysis software in this research (except for glucose) were slightly higher than those obtained from the values of T_f' determined by the method of Richardson and Savill [32].

In general, it was found that the T_f' of the unaged sugars was between the T_g onset and T_g midpoint. This result was similar to that reported by Lammert *et al.* [11] for the physical ageing of maltose glasses. However, the T_f' value of glucose was slightly lower than its T_g onset. Schmidt and Lammert [12] found that T_f' value of a maltose glass using an equal heating rate and cooling rate of 10°C min^{-1} was also slightly lower than T_g onset. Montserrat [25] reported that the value of T_f' (98.3°C) for a fully cured epoxy resin based on diglycidyl ether of bisphenol was in good agreement with the T_g midpoint (98.3°C) determined from the unaged DSC scan.

Aged sugars

The fictive temperature of the aged glasses, T_f, was obtained from the intersection of the extrapolated glass and liquid enthalpy curves [32]. As physical ageing proceeds, T_f is expected to decrease as ageing time increases due to a decrease in enthalpy as the sample approaches equilibrium. This is confirmed by the results shown in Fig. 6. The decrease of T_f as a function of ageing time is self-retarding which is a well-known characteristic of structural relaxation and has also been found in maltose glasses [11], and in polymers such as phenolphthalein poly(aryl-ether-ketone) and poly(aryl-ether-sulfone) [37].

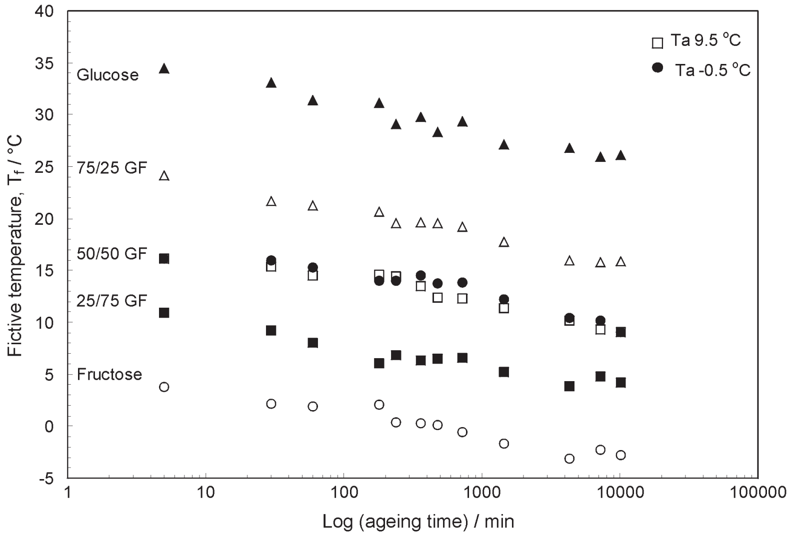

Fig. 6 The fictive temperatures (T_f) analyzed by the method of Richardson and Savill [32] for glucose, fructose, and three mass ratios of glucose to fructose; 75/25, 50/50 at two ageing temperatures (9.5 and –0.5°C), and 25/75 as function of ageing time

Between the two ageing temperatures (9.5 and –0.5°C) for 50/50 GF, it is expected that the T_f of the sample aged at –0.5°C would be higher than that aged at 9.5°C (Fig. 6) because the structural relaxation slows down as the ageing temperature decreases. This can be seen more clearly in the T_g plots (Figs 3a to 3c), but is not as obvious in the T_f plot (Fig. 6). Overall, the T_f values for the samples aged at –0.5°C were slightly higher than the values for the samples aged at 9.5°C. For both ageing temperatures, T_f decreased rapidly for the first 2000 min, but as the self-retarding processed, the decrease in T_f slowed down, as shown in Fig. 6 (note log scale on x-axis). In polymers, the higher the ageing temperature, the faster the decrease in T_f, because the packing of molecular chains is accelerated at higher ageing temperatures [37]. However, at longer ageing times, the rate of ageing was much slower at both ageing temperatures because of the stronger dependence of the ageing rate on the distance from equilibrium. Therefore, for the 50/50 GF samples, both T_f for the higher and lower ageing temperatures approached nearly the same value (about 10°C). Theoretically, T_f will be equal to T_a when the sample is aged until it reaches equilibrium (Fig. 1). If the T_f is observed for ageing times much longer than the experimental time scale used in this research, it is expected that the T_f of the higher ageing temperature will reach equilibrium with an approximate value of $T_f=T_a=9.5$°C. The T_f for the –0.5°C ageing temperature decreased at a much slower rate than the 9.5°C ageing temperature until it reached equilibrium at around –0.5°C (corresponding to $T_f=T_a$).

Bauwens-Crowet and Bauwens [38–40] showed that the slope of the plot of the relaxation enthalpy at equilibrium, ΔH_∞, *vs.* T_f in aged polycarbonate (PC) was equal to the mean value of ΔC_p of the sample. The value of the unaged limiting fictive temperature or T_f' was obtained by extrapolation to zero ΔH_∞ on the same graph. T_f in their case was the fictive temperature at equilibrium enthalpy, therefore, T_f and T_a were equal. Note that the terms structural temperature, θ, and unannealed structural temperature, θ_i, were used in the original paper, instead of T_f and T_f' respectively. The value of θ_i and ΔC_p from the graph were found to fit the relation $\Delta H=\Delta C_p(\theta-\theta_i)$. Note that in contrast to the present research, the Bauwens-Crowet and Bauwens [38] paper defined ΔH as the unaged (reference) DSC curve minus the aged curve. Claudy *et al.* [41] also showed a similar relation in a glycerol glass:

$$\Delta H \approx \Delta C_p (T_f' - T_f) \tag{4}$$

Two plots between the relaxation enthalpy and the fictive temperature of Eq. (4) are shown in Fig. 7. The solid lines are the linear least squares fit to the raw (ΔH and T_f) data. The resulting linear equations are given in Fig. 7. The absolute value of the slopes (ΔC_p) for glucose, 75/25 GF, 50/50 GF aged at 9.5°C and –0.5°C, 25/75 GF and fructose were 0.78, 0.83, 0.80, 1.05, 0.86, and 0.85, respectively. The dashed lines show values for ΔH calculated from Eq. (4) using the experimental values for ΔC_p (average unaged, Table 2) and T_f (Fig. 6).

The ΔC_p values obtained from the linear least squares fit (the slopes of the solid lines), in general, were higher than the experimental of the average unaged ΔC_p values given in Table 2. The difference between the experimental ΔC_p (Table 2) and approximated ΔC_p values (Eq. (4)) may be due to the relation in Eq. (4) being only an

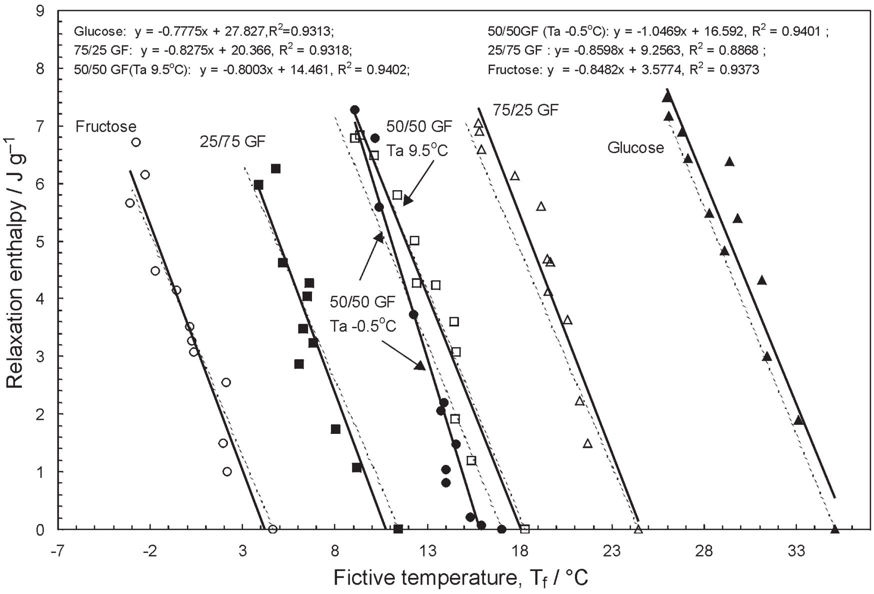

Fig. 7 Linear relationship of the relaxation enthalpy, ΔH, as a function of fictive temperature of the sugars. The solid line is the linear least squares fit of the raw (ΔH and T_f) data. The resulting linear equations are given on the graph. The dashed lines show values for ΔH calculated from Eq. (4) using the experimental values for ΔC_p (average unaged, Table 2) and T_f (Fig. 6)

approximation. In order to obtain accurate ΔC_p values via Eq. (4) using ΔH and T_f data, accuracy in the determination of ΔH and T_f is required. Cowie and Ferguson [28] found that the range of the two integral limits (given in Table 2 for this research) could affect the value of ΔH obtained experimentally. In general, a larger experimental error was observed in the measurement of relaxation enthalpy than in that of excess volume for volume relaxation experiments [1]. A slight error in the determination of T_f might occur because this value was extrapolated from the liquid and glassy enthalpy curves. Also since the aged T_f values were measured during heating, they may be affected by possible relaxation during cooling from the ageing temperature to the starting temperature of the reheating scan [42]. However, under the limitations of experimental error, the first approximation of the relation between ΔH and fictive temperature for the sugars can be obtained via Eq. (4), as shown by the close proximity of the dashed line (calculated using Eq. (4)) and the solid lines (obtained from the linear least squares fit to the raw data ΔH and T_f) in Fig. 7.

Kinetics of ageing

When a sugar is cooled from the liquid state through its T_g, the non-equilibrium nature of the transition causes the material to deviate from the equilibrium liquidus line (Fig. 1). As the amorphous sugar glass is aged at a constant ageing temperature below its T_g, the enthalpy of the glass relaxes toward equilibrium, i.e., the enthalpy decreases as ageing time increases. As the glass is reheated, the enthalpy increases and crosses the equilibrium liquidus line. The endothermic peak observed on the heating DSC curve is known as the T_g overshoot and is the recovery of the enthalpy which was lost during the ageing process below T_g. This T_g overshoot is typical of all aged polymers. The intensity and position of the T_g overshoot was reported for a variety of polymers such as epoxy resins, polyetherimide, and amorphous polyester, and is dependent on ageing temperature and ageing time [25, 43–46]. Although it was assumed that no appreciable ageing occurred during cooling of the sample (from T_g to T_a and from T_a to the starting rescan temperature) and during equilibrating step (at the starting rescan temperature, as mentioned in the method section), a small T_g overshoot was observed on the heating rescan of unaged glucose. This suggests that some relaxation occurred during these cooling and equilibrating steps. The decrease of the unaged T_g overshoot with increasing fructose content indicates that the relaxation of fructose was much slower than that of glucose during the cooling and equilibrating steps.

It is well recognized that the physical ageing phenomena can be described more accurately when the concept of a distribution of relaxation times is introduced into a relaxation function. To date, the most widely used relaxation function for structural relaxation is the stretched exponential function referred to as the Kohlrausch–Williams–Watts (KWW) function [47–50]:

$$\phi(t) = f(t,\tau) = \exp(-(t/\tau)^{\beta}) \tag{5}$$

where $\phi(t)$ is the relaxation function, τ is the characteristic relaxation time, and β is a parameter characterizing the width of the relaxation time distribution spectrum ($0\leq\beta\leq1$). A small value of β implies a very broad distribution, and a β value close to unity implies a very narrow distribution of relaxation times [28]. This semi-empirical function is used to describe isothermal enthalpy relaxation at a given ageing temperature T_a for a given ageing time t_a. In the Cowie and Ferguson (CF) model [10, 28, 51–54], the relaxation function, $\phi(t)$, is defined in terms of the excess enthalpy as:

$$\phi(t) = \frac{H(t) - H_\infty}{H_{\mathrm{to}} - H_\infty} = \frac{\delta_{\mathrm{H}}}{\Delta H_\infty} = 1 - \frac{\Delta H(t)}{\Delta H_\infty} \tag{6}$$

where H_{to} is the enthalpy at zero ageing time, $H(t)$ and H_∞ are the enthalpy at ageing time t and at infinite time (equilibrium enthalpy). The quantity $H(t)–H_\infty$ is referred to as the excess enthalpy, δ_{H}, which is also equal to $H(t)–H_\infty$ [55]. By combining Eqs (5) and (6) and rearranging, $\Delta H(t)$ can be rewritten as:

$$\Delta H(t) = \Delta H_\infty = \left[1 - \exp\left[-\left(\frac{t}{\tau}\right)\right]^{\beta}\right] \tag{7}$$

In the original CF model equation, t_c was used instead of τ to indicate that this characteristic time is a constant. It should be pointed out that the CF model treats the characteristic time, τ, as a constant, in other word, the time dependence of τ is ignored. The accuracy of the parameters obtained from the CF model has been questioned because the time dependence of τ is not taken into account [42, 56]. However, Cowie and Ferguson [52, 53] showed that there was no significant improvement in the fitting of the data (all significance levels >0.05) between the original CF model and a modified version of the CF model which accounted for the time-dependent characteristic of τ in poly(methyl methacrylate). The reliability of the CF model for fitting real data was also illustrated in the paper by Brunacci *et al.* [57]. They noted that the CF model was employed as a means of obtaining information about the long-ageing-time behavior of polymer glasses which most of the other models do not consider. For the interested reader, Wungtanagorn and Schmidt [58] investigated the time-dependent characteristic of τ in glucose/fructose systems.

The solution of Eq. (7) (ΔH_∞, τ and β) was obtained using a non-linear least squares fitting analysis in the Microsoft Excel Solver software. The software minimized the sum of squares of the residuals (SS) which was calculated from the sum of the difference between the experimental and calculated $\Delta H(t)$ values:

$$SS = \sum_{i=1}^{n} (\Delta H(t)_i^{\mathrm{exp}} - \Delta H(t)_i^{\mathrm{cal}})^2 \tag{8}$$

where $\Delta H(t)_i^{\mathrm{exp}}$ and $\Delta H(t)_i^{\mathrm{cal}}$ are the experimental and calculated enthalpy, respectively.

In the case of the 50/50 GF sample aged at –0.5°C, the value of ΔH_∞ could not be obtained accurately by the fitting method because the time scale of this experiment was much shorter than the time required to reach equilibrium. The value of ΔH_∞ in that case was, therefore, obtained by extrapolating the liquid enthalpy curve of the reference unaged sample to below the glass transition temperature and the $\Delta H_\infty(T_a)=H(T_a)_{\mathrm{glass}}-H(T_a)_{\mathrm{liquid}}$. $\Delta H_\infty(T_a)$ can be rewritten in the term of the heat capacity as shown in Eq. (9) [28, 51, 52]:

$$\Delta H_\infty(T_a) = \int_{T_a}^{T>T_g} [C_p(T')_{\mathrm{liquid}} - C_p(T')_{\mathrm{unaged}}]\mathrm{d}T' \tag{9}$$

The upper limit of the integral was taken at least 30°C above T_g midpoint. $C_p(T')_{\mathrm{liquid}}$ is a linear least-squares fit to the heat capacity of the unaged sample in the liquid state, and $C_p(T')_{\mathrm{unaged}}$ is the heat capacity obtained from the unaged sample from the experiment.

The CF model parameters obtained for the aged sugar glasses are given in Table 5. The enthalpy relaxation data for the aged sugar glasses were plotted as a function of ageing time and were fit to the CF model (Eq. (7)) represented by the lines in Fig. 8. The 5 min data was not included in this analysis because the change in enthalpy (ΔH) was too small to be detected accurately. The uncertainties of the parameters in Table 5 do not represent the actual uncertainties of the parameters on fitting. The actual uncertainties can be obtained but a very long experimental time scale is necessary because replication of each data point is required. In this experiment, only the samples with short ageing times (up to 360 min) were duplicated. The uncer-

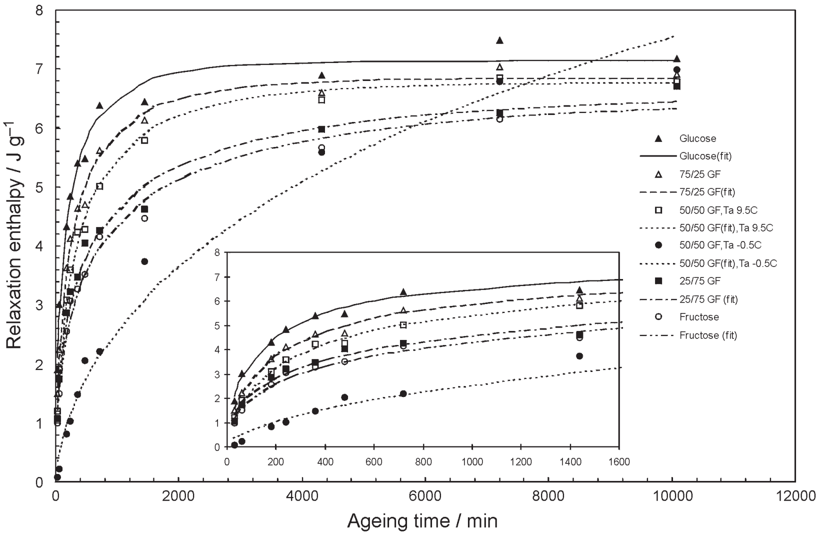

Fig. 8 Relaxation enthalpy data ($\Delta H(t)$, J g^{-1}) as a function of ageing time for sugar samples aged from 30 min to 7 days (10 080 min). The ageing temperatures of 28.0, 16.5, 4.5 and –2.0°C were used for glucose, 75/25 GF, 25/75 GF, and fructose, respectively. Two ageing temperatures of 9.5 and –0.5°C were used for the 50/50 GF sample. The lines are the Cowie and Ferguson model fits (Eq. (7)) to the experimental enthalpy relaxation data. The scale of ageing time from 0 to 1600 min was magnified in the insert

tainties of each parameter in Table 5 were estimated by changing the values of that parameter while the others remained constant so that the minimum sum of squares of the residues (Eq. (8)) was doubled. These uncertainties actually have no real significance but only show the sensitivity of the response of each parameter to the fitting. In agreement with the report on ageing of polystyrene by Agrawal [59], the sum of squares changed abruptly with a small change in the parameters ΔH_∞ and β, while it was less sensitive to t_c.

Table 5 Cowie and Ferguson model parameters of aged sugars obtained by non-linear least squares fitting of the experimental $\Delta H(t)$ to the CF model (Eq. (7)). ΔH_∞ of the 50/50 GF sample aged at –0.5°C was calculated using Eq. (9)

Sample	Ageing temp./ °C	T_g midpoint– T_a/ °C	ΔH_∞/ J g^{-1}	t_c/min	β
Glucose	28.0	9.89	7.14±0.126	201.8±17.68	0.56±0.054
75/25 GF	16.5	10.14	6.86±0.098	302.9±19.59	0.57±0.039
50/50 GF	9.5	10.75	6.79±0.168	420.6±50.38	0.58±0.066
50/50 GF	–0.5	19.47	14.28±0.628	16301.8±4458.24	0.58±0.038
25/75 GF	4.5	8.61	6.66±0.209	704.7±104.050	0.47±0.052
Fructose	–2.0	8.78	6.60±0.247	855.9±168.11	0.48±0.062

The β values for the sugars in this study ranged from 0.47 to 0.58 (Table 5). The β values of other sugars have been reported: for sucrose between 0.4 to 0.8 by Handcock *et al.* [14], and 0.33 by Urbani *et al.* [13], and for maltose at 0.41±0.021 by Schmidt and Lammert [12] and 0.32 to 0.44 by Lammert *et al.* [11]. The characteristic relaxation time of maltose (about 660–800 min) was similar to that of fructose, but higher than that of glucose at T_a approximately 10°C below T_g. The increase in the relaxation time t_c as the ratio of fructose increased (Table 5) indicates that fructose slowed the relaxation toward equilibrium in the mixtures. The values of ΔH_∞ obtained from fitting to the CF model decreased slightly as the ratio of fructose increased. In the case of the 50/50 GF sample aged at –0.5°C, the experimental data was not fit very well by the CF model. This is probably because of the approximate nature of the calculated ΔH_∞ via Eq. (9). The value of ΔH_∞ actually should be treated as an adjustable parameter in the CF model when the ageing temperature is near T_g and long experimental time scales are used. As pointing out by Hutchinson [1], evaluation of ΔH_∞ is a major problem in the study of enthalpy relaxation. Enthalpy equilibrium can be achieved experimentally only in the limiting range of ageing temperatures below the glass transition temperature and equilibrium will never be achieved within an accessible time at lower ageing temperatures. In this experiment, ageing at approximately 10°C below the midpoint glass transition temperature (and even closer to the onset temperature) is quite reasonable for nearly obtaining equilibrium in 7 days. However, a much longer experimental time scale is needed for the –0.5°C aged sample in order to obtain an accurate ΔH_∞ value.

If the non-exponential relaxation function, $\phi(t)$, is considered to arise from a superposition of exponentials, i.e., a summation of many different elementary processes, where each elementary process is subject to a single relaxation time, τ [60, 28], then $\phi(t)$ can be expressed in the integral form as:

$$\phi(t) = \exp(-t/\tau)^{\beta} = \int_0^\infty \exp(-t/\tau)\rho(\tau)\mathrm{d}\tau \tag{10}$$

where $\rho(\tau)$ is the distribution of relaxation times. $\rho(\tau)$ is the Dirac δ function when β is unity. It is possible to find the average relaxation time, $<\tau>$, without explicit knowledge of $\rho(\tau)$. The average relaxation time, $<\tau>$, for the KWW distribution, is given by [28, 60–62]:

$$\langle\tau\rangle = \frac{\tau}{\beta}\Gamma\left(\frac{1}{\beta}\right) \tag{11}$$

where Γ is the gamma function. Parameter τ is the parameter t_c in the CF model. The average relaxation time $<\tau>$ is t_c when β equals 1. The parameter $<\tau>^{-1}$ is proportional to the ageing rate of the sugar glasses. In addition, $<\tau>^{-1}$ can be related to ΔH_∞ and T_a, in order to characterize the ageing behavior, by means of the entropy production parameter, P, which is defined as [46]:

$$P = \frac{\Delta H_{\infty}}{T_{\mathrm{a}}} \langle\tau\rangle^{-1} \qquad (12)$$

where $\Delta H_{\infty}/T_{\mathrm{a}}$ is the thermodynamic driving force for the ageing process. The entropy production parameter indicates how fast the system relaxes toward equilibrium, i.e., the higher the P parameter, the faster the system progresses toward equilibrium.

The values of $<\tau>$ and P for the sugars are given in Table 6. The increase of $<\tau>$ (or the decrease of $<\tau>^{-1}$) and the decrease of entropy production parameter as the content of fructose increases clearly indicated that the ageing rate decreases with increasing the fructose content in the sugar system.

Table 6 The average relaxation time ($<\tau>$) and entropy production parameter (P) defined by Eq. (12) of glucose, fructose, and their mixtures

Sugars	Fructose mass ratio	$<\tau>$, min	$P \cdot 10^5$, J g^{-1} K^{-1} min^{-1}
Glucose	0.00	338.66	7.00
75/25 GF	0.25	486.84	4.86
50/50 GF aged at 9.5°C	0.50	668.74	3.59
50/50 GF aged at –0.5°C	0.50	25535.33	0.21
25/75 GF	0.75	1612.23	1.49
Fructose	1.00	1894.19	1.29

Experimental techniques for microstructural analysis during physical ageing of polymers were reviewed by Hutchinson [1]. The observations from microstructural studies can, in general, be rationalized using the concepts of free volume and free volume distribution; although, some of the observations cannot neatly be rationalized on the basis of free volume. A polymer accommodates the change in temperature from above its T_g to below its T_g by physically rearranging its molecules. Upon cooling below the transition range, the polymer becomes a glass with no additional rearrangement [63] or in other words the structure of the glass is frozen-in [1]. To our knowledge, changes in microstructure for simple sugars during physical ageing have not been previously reported. One, however, may apply this same concept for polymers to the case of simple sugars.

Sugar crystals are melted at or above their specific melting temperature to form a molten sugar. As noted by Fan and Angell [23], the melting of sugar is not a well-defined process because the liquid formed immediately on melting is not an equilibrium state of the system. A sugar in the molten state, above its T_g, is composed of more than one conformer (epimers, tautomers, and anomers). The rate at which equilibrium is reached and the equilibrium composition of the conformers depend on temperature, initial sugar concentration, and solvent [64]. The interconversion amongst conformers occurs until equilibrium is reached at a given temperature. The equilibrium mixture of glucose only contains two anomeric forms of $^1C_4$ pyranoid ring (i.e. α-*D*-glucopyranose and β-*D*-glucopyranose) while the equilibrium mixture

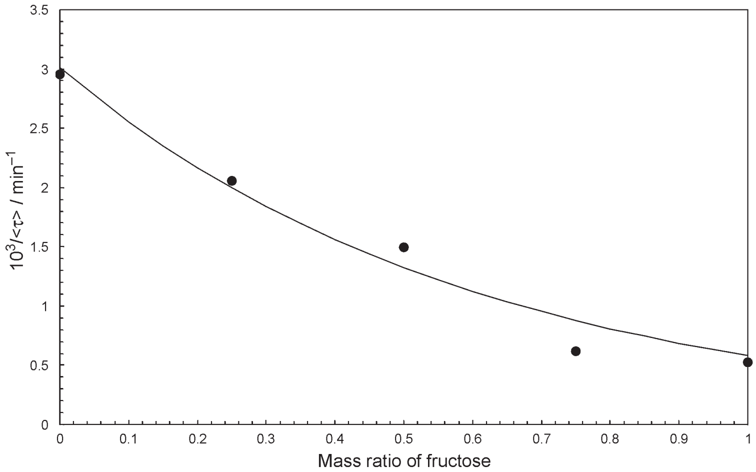

Fig. 9 The value of $<\tau>^{-1}$ as a function of mass fraction of fructose in the sugar mixtures. The line is the exponential fit of the experimental data to Eq. (13)

of fructose contains at least six distinct species (i.e. the two anomeric forms of each of $^1C_4$ and $^4C_1$ and of furanose ring) [64].

The conformer concentration is frozen-in when the molten sugar is cooled to a temperature below its T_g. The ageing process is considered to be the release of the frozen-in molecular motions [1]. At a constant temperature below T_g and as time is allowed for the frozen-in molecular motions to be released, a transition from one conformer to another may occur until equilibrium amongst the conformers at that temperature is reached. Since the phenomenon of physical aging is manifested as a reduction in volume (and enthalpy), the interconversion amongst the conformers in sugar glasses may be related to the minimum packing of the molecules and a decrease in the free volume of sugars during aging. Because only two major conformers coexist in glucose glasses, it is expected that the equilibrium state of the glucose glass should be reached faster than that of the fructose glass which is composed of at least six conformers. To confirm this hypothesis, changes in the conformer concentration of both glucose and fructose as a function of aging time and temperature should be investigated. Solid state NMR of the sugars over times may be one possible method of use for such a study.

By using the published values of the CF parameters for maltose by Schmidt and Lammert [12] and Lammert *et al.* [11], the values of $<\tau>$ and enthalpy production were calculated: for $<\tau>$, 1724.88 (equal heating rate at 10°C min^{-1} and ageing at T_g–10.8°C), 570148.3 (equal heating rate at 10°C min^{-1} and ageing at T_g–20.8°C), and 423.77 min (heating rate at 10°C min^{-1} and quench cooling), and for enthalpy production, $1.435 \cdot 10^5$ (equal heating rate at 10°C min^{-1} and ageing at T_g–10.8°C), $0.0082 \cdot 10^5$ (equal heating rate at 10°C min^{-1} and ageing at T_g–20.8°C), and $5.465 \cdot 10^5$ J g^{-1} K^{-1} min^{-1} (heating rate at 10°C min^{-1} and quench cooling). The $<\tau>$ and P values for maltose are in a similar range to that of glucose and fructose (Table 6).

Pauly and Kammer [46] studied the effect of acrylonitrile (AN) content on the physical ageing in copolymers of styrene and acrylonitrile (SAN). Their data showed that an exponential relationship between the ageing rate $<\tau>^{-1}$ and the mass ratio of the AN content in SAN could be approximated by:

$$\langle\tau\rangle^{-1} = \langle\tau\rangle_{\mathrm{o}}^{-1}\mathrm{e}^{-\mathrm{w/w_o}} \tag{13}$$

where w is the AN content, w_{o} and $\langle\tau\rangle_{\mathrm{o}}^{-1}$ are constants. In this research, Eq. (13) was also used to approximate the relation of $<\tau>^{-1}$ and the mass ratio of fructose content, w. The calculated $<\tau>^{-1}$ data from Table 6 were fit to Eq. (13) using a non-linear least squares fitting method. The total sum of square of the difference between experimental $<\tau>^{-1}$ and calculated $<\tau>^{-1}$ was minimized. The values of $\langle\tau\rangle_{\mathrm{o}}^{-1}$ and w_{o} from the fitting were found to be $3.016 \cdot 10^3$ min^{-1} and 0.593, respectively (with the sum of squares of 0.11). Good agreement between the experimental $<\tau>^{-1}$ (indicated by points) and the calculated $<\tau>^{-1}$ (via Eq. (13), the solid line) values is shown in Fig. 9.

Conclusions

It has been shown that the glass transition and fictive temperatures of glucose, fructose, and their mixtures were affected by the ageing process. The DSC glass transition temperatures slightly increased, whereas the fictive temperatures decreased with increasing ageing time. The glass transition temperature range determined by the onset minus the endpoint glass transition temperatures was narrower in the unaged samples as the content of fructose increased and in aged samples as the ageing time increased. The existence of high-temperature transitions above T_{g} was confirmed in fructose. These transitions became smaller with the decrease in fructose content in the glucose–fructose mixtures and were not effected by the ageing process below the glass transition temperature. A rough approximation of enthalpy relaxation can be obtained from the fictive temperature and heat capacity data. In conjunction with the Cowie and Ferguson model, the characteristic relaxation time increased with increasing fructose content in the mixtures. The increase in the relaxation time as the ratio of fructose increased indicated that fructose slowed down the relaxation toward equilibrium in the mixtures. The development of enthalpy relaxation was affected by the ageing temperature, i.e., the lower the ageing temperature, the longer the relaxation time and, therefore, the slower the system progressed toward equilibrium. The average relaxation time, $<\tau>$, and entropy production parameter, P, confirmed that fructose decreased the rate of ageing. The value of $<\tau>^{-1}$ was calculated at various mass fractions of fructose via the simple exponential Eq. (13).

* * *

It is a pleasure to acknowledge that the HPLC glucose–fructose ratio analysis and the Karl–Fischer moisture content analysis were done by A. E. Staley Manufacturing Company, Decatur, IL.

References

1 J. M. Hutchinson, Polym. Prog. Polym. Sci., 20 (1995) 703.
2 L. C. E. Struik, Physical ageing in Amorphous Polymers and Other Materials, Elsevier Scientific Publishing Company, New York 1978.
3 A. Tanaka, K. Nitta, R. Maekawa, T. Masuda and T. Higashimura, Polym. J., 24 (1992) 1173.
4 S. Mukherjee and S. A. Jabarin, Polym. Engineering Sci., 35 (1995) 1145.
5 V. T. Troung and B. C. Ennis, Polym. Engineering and Sci., 31 (1991) 548.
6 J. C. Arnold, Polym. Engineering Sci., 35 (1995) 165.
7 A. C. M. Yang, R. C. Wan and J. J. Jin, Polym., 37 (1996) 5751.
8 J. K. Hebb, K. E. Sykes, T. J. McMaster and P. J. Barham, J. Environmental Polym. Degradation, 4 (1996) 235.
9 C. M. Ma, C. Lee, M. Chang and N. Tai, Polym. Composites, 13 (1997) 441.
10 J. M. G. Cowie and R. Ferguson, Polym. Comm., 27 (1986) 258.
11 A. M. Lammert, R. M. Lammert and S. J. Schmidt, J. Therm. Anal. Cal., 55 (1999) 949.
12 S. J. Schmidt and A. M. Lammert, J. Food Sci., 61 (1996) 870.
13 R. Urbani, F. Sussich, S. Prejac and A. Cesaro, Thermochim. Acta, 304/305 (1997) 359.
14 B. C. Handcock, S. L. Shamblin and G. Zografi, Pharm. Res., 12 (1995) 799.
15 M. E. Sahagian and H. D. Goff, Food Res. Int., 28 (1995) 1.
16 M. E. Sahagian and H. D. Goff, Thermochim. Acta, 246 (1994) 271.
17 M. Le Meste, G. Roudaut and S. Davidou, J. Thermal Anal., 47 (1996) 1361.
18 Corn Refiners Association, Inc., Standard Analytical Methods. Method E-46, 1100 Connecticut Avenue, NW., Washington, D.C. 20036 (1992).
19 Y. Roos, Carbohydr. Res., 238 (1993) 39.
20 A. Raemy, R. F. Hurrell and J. Loliger, Thermochim. Acta, 65 (1983) 81.
21 L. Slade and H. Levine, Pure Appl. Chem., 60 (1988) 1841.
22 CRC Handbook of Chemistry and Physics. 78th Edition. D.R. Lide (Ed.). CRC Press, Boca Raton, New York 1997–1998.
23 J. Fan and C. A. Angell, Thermochim. Acta, 266 (1995) 9.
24 R. R. Lagasse, J. Polym. Sci. Polym. Phys., 20 (1982) 279.
25 S. Montserrat, J. Polym. Sci. Polym. Phys., 32 (1994) 509.
26 TA Instruments, Thermal Solutions: Heat Capacity Analysis Manual. PN 925635.002 Rev. B. New Castle, DE., 1997.
27 TA Instruments, Universal Analysis Operator’s Manual. PN 925609.002. New Castle, DE., 1996.
28 J. M. G. Cowie and R. Ferguson, Macromolecules, 22 (1989a) 2307.
29 A. Q. Tool, J. Am. Ceram. Soc., 29 (1946) 240.
30 O. S. Narayanaswamy, J. Am. Ceram. Soc., 54 (1971) 491.
31 C. T. Moynihan, A. J. Easteal, M. A. DeBolt and J. Tucker, J. Am. Ceram. Soc., 59 (1976) 12.
32 M. J. Richardson and N. G. Savill, Polym., 16 (1975) 753.
33 P. D. Orford, R. Parker and S. G. Ring, Carbohydr. Res., 196 (1990) 11.
34 L. Finegold, F. Franks and R. H. M. Hatle, J. Chem. Soc. Faraday Trans., 85 (1989) 2445.
35 P. R. Couchman and F. E. Karasz, Macromolecules, 11 (1978) 117.
36 R. Wungtanagorn. Ph.D. Thesis, 2000, University of Illinois at Urbana-Champaign.
37 Y. Di, A. D’Amore, G. Marino, L. Nicolais and B. Li, J. Appl. Polym. Sci., 57 (1995) 989.
38 C. Bauwens-Crowet and J. C. Bauwens, Polym., 23 (1982) 1599.

39 C. Bauwens-Crowet and J. C. Bauwens, Polym., 27 (1986) 709.

40 C. Bauwens-Crowet and J. C. Bauwens, J. Non-Cryst. Solids., 131–133 (1991) 505.

41 P. Claudy, S. Jabrane and J. M. Letoffe, Thermochim. Acta., 293 (1997) 1.

42 I. M. Hodge, J. Non-Cryst. Solids, 169 (1994) 211.

43 W. D. Cook, M. Mehrabi and G. H. Edward, Polym., 40 (1999) 1209.

44 I. Echeverria, P. Su, S. L. Simon and D. J. Plazek. J. Polym. Sci. Polym. Phys., 33 (1995) 2457.

45 P. Cortes and S. Montserrat, J. Non-Cryst. Solids, 172-174 (1994) 622.

46 S. Pauly and K. W. Kammer, Polym. Networks Blends, 4 (1994) 93.

47 R. Kohlrausch, Pogg. Ann. Phys., 91 (1854) 198; J. M. Hutchinson, Prog. Polym. Sci., 20 (1995) 703.

48 R. Kohlrausch, Pogg. Ann. Phys., 119 (1863) 352; J. M. Hutchinson, Prog. Polym. Sci., 20 (1995) 703.

49 G. Williams and D. C. Watts, Trans. Faraday Soc., 66 (1970) 80.

50 G. Williams, D. C. Watts, S. B. Dev and A. M. North, Trans. Faraday. Soc., 67 (1971) 1323.

51 J. M. G. Cowie and R. Ferguson, Macromolecules, 22 (1989b) 2312.

52 J. M. G. Cowie and R. Ferguson, Polym., 34 (1993) 2135.

53 J. M. G. Cowie and R. Ferguson, Polym., 36 (1995) 4159.

54 J. M. G. Cowie, S. Elliott, R. Ferguson and R. Simha, Polym., Comm., 28 (1987) 298.

55 S. C. Jain and R. Simha, Macromolecules, 15 (1982) 1522.

56 I. M. Hodge and J. M. O’Reilly, Polym., 33 (1992) 4883.

57 A. Brunacci, M. G. Cowie, R. Ferguson and I. J. McEwen, Polym., 38 (1997) 865.

58 R. Wungtanagorn and S. J. Schmidt, Themochim. Acta, (accepted October 2000).

59 A. Agrawal, J. Polym. Sci. Polym. Phys., 27 (1989) 1449.

60 C. P. Lindsey and G. D. Petterson, J. Chem. Phys., 73 (1980) 3348.

61 C. T. Moynihan, L. P. Boesch and N. L. Laberge, Phys. Chem. Glasses, 14 (1973) 122.

62 F. L. Cumbrera, F. Sanchez-Bajo, F. Guiberteau, J. D. Solier and A. Munoz, J. Mat. Sci., 28 (1993) 5387.

63 S. Brawer, Relaxation in Viscous Liquids and Glasses: Review of Phenomenology, Molecular Dynamics Simulations, and Theoretical Treatment, The American Ceramic Society, Inc., Columbus, Ohio 1985, p. 5.

64 F. Frank, Pure Appl. Chem., 59 (1987) 1189.

65 P. D. Orford, R. Parker, S. G. Ring and A. C. Smith, Int. J. Biol. Macromolecules, 11 (1989) 91.

66 A. L. Ollett and R. Parker, J. Texture Stud., 21 (1990) 355.